Vibrational Spectroscopy 66 (2013) 69–75

Contents lists available at SciVerse ScienceDirect

Vibrational Spectroscopy

journal homepage: www.elsevier.com/locate/vibspec

Vibrational spectroscopic characterization of the phosphate mineral hureaulite – $(Mn, Fe)_5(PO_4)_2(HPO_4)_2{\cdot}4(H_2O)$

Ray L. Frost[a,*], Yunfei Xi[a], Ricardo Scholz[b], Andrés López[a], Fernanda M. Belotti[c]

[a] School of Chemistry, Physics and Mechanical Engineering, Science and Engineering Faculty, Queensland University of Technology, GPO Box 2434, Brisbane, Queensland 4001, Australia
[b] Geology Department, School of Mines, Federal University of Ouro Preto, Campus Morro do Cruzeiro, Ouro Preto, MG 35,400-00, Brazil
[c] Federal University of Itajubá, Campus Itabira, Itabira, MG 35,903-087, Brazil

ARTICLE INFO

Article history:
Received 22 May 2012
Received in revised form 3 February 2013
Accepted 11 February 2013
Available online 18 February 2013

Keywords:
Raman spectroscopy
Hureaulite
Infrared spectroscopy
Phosphate
Pegmatite

ABSTRACT

This research was done on hureaulite samples from the Cigana claim, a lithium bearing pegmatite with triphylite and spodumene. The mine is located in Conselheiro Pena, east of Minas Gerais. Chemical analysis was carried out by Electron Microprobe analysis and indicated a manganese rich phase with partial substitution of iron. The calculated chemical formula of the studied sample is: $(Mn_{3.23}, Fe_{1.04}, Ca_{0.19}, Mg_{0.13})(PO_4)_{2.7}(HPO_4)_{2.6}(OH)_{4.78}$. The Raman spectrum of hureaulite is dominated by an intense sharp band at 959 cm^{-1} assigned to PO stretching vibrations of HPO_4^{2-} units. The Raman band at 989 cm^{-1} is assigned to the PO_4^{3-} stretching vibration. Raman bands at 1007, 1024, 1047, and 1083 cm^{-1} are attributed to both the HOP and PO antisymmetric stretching vibrations of HPO_4^{2-} and PO_4^{3-} units. A set of Raman bands at 531, 543, 564 and 582 cm^{-1} are assigned to the ν_4 bending modes of the HPO_4^{2-} and PO_4^{3-} units. Raman bands observed at 414, and 455 cm^{-1} are attributed to the ν_2 HPO_4^{2-} and PO_4^{3-} units. The intense A series of Raman and infrared bands in the OH stretching region are assigned to water stretching vibrations. Based upon the position of these bands hydrogen bond distances are calculated. Hydrogen bond distances are short indicating very strong hydrogen bonding in the hureaulite structure. A combination of Raman and infrared spectroscopy enabled aspects of the molecular structure of the mineral hureaulite to be understood.

1. Introduction

Hureaulite is a manganese hydrated acid phosphate mineral with general chemical formula expressed by $(Mn, Fe)_5(PO_4)_2(HPO_4)_2{\cdot}4(H_2O)$. It was first discovered and named by Alluaud [1] in 1826 in samples from Huréaux quarry, St. Sylvestre, Haute-Vienne, France, and was first described by Dufrénoy in 1829 [2]. The mineral belongs to the hureaulite group that also includes: miguelromeroite [3], nyholmite [4], sainfeldite [5] and villyaellenite [6]. A comparison among the members of the hureaulite group suggest a general chemical formula expressed by $(M1)(M2)_2(M3)_2(XO_4)_2(HXO_4)_2{\cdot}4(H_2O)$, where M1 = Mn, Ca, Cd; M2 = Fe, Mn, Cd, Ca; M3 = Fe, Mn, Zn, Ca and X can be occupied by P and As.

The crystal structure of hureaulite was solved by Moore and Araki [7]. The mineral crystallizes in monoclinic crystal system, $C2/c$ space group with unit-cell parameters $a = 17.594(10)$ Å, $b = 9.086(5)$ Å, $c = 9.404(5)$ Å, $\alpha = 90°$, $\beta = 96.67(8)°$, $\gamma = 90°$, $V = 1493.14$ Å^3 and $Z = 4$. Hureaulite structure consists of an open three-dimensional network formed by octahedral pentameric entities that share vertices with the $[PO_4]$ and $[PO_3(OH)]$ tetrahedra. Mössbauer spectroscopy characterization was carried out by Moreira et al. [8], who described a complete Mn^{2+}–Fe^{2+} solid solution.

Hureaulite is a common mineral in lithium bearing pegmatites and is related to the hydrothermal alteration after triphylite–lithiophilite or some other Fe–Mn primary phosphate. Hureaulite also can originate from the hydrothermal reaction of Mn-rich phosphatic solutions. Moore described hureaulite as an early to late hydrothermal mineral in the phosphate paragenesis of granitic pegmatites [9]. Hureaulite has been synthesized by different methods. Hydrothermal synthesis and treatment in different physical and chemical conditions were used to obtain single and doped hureaulite crystals [10–12]. In recent studies, hureaulite crystals have produced by reflux process at ambient temperature and pressure [13–15].

Hureaulite has potential to application in different ways in industry, such as magnetics, optics, and electrochemistry. In addition, hureaulite is widely used as an additive to obtain highly corrosion-resistant surfaces in order to improve the wear resistance of steels (3, 7, 8, 9). A dense, finely-structured phosphate layer firmly attaches to the substrate when hureaulite is

* Corresponding author. Tel.: +61 7 3138 2407; fax: +61 7 3138 1804.
E-mail address: r.frost@qut.edu.au (R.L. Frost).

0924-2031/$ – see front matter © 2013 Elsevier B.V. All rights reserved.
http://dx.doi.org/10.1016/j.vibspec.2013.02.003

used to form corrosion-resistant surfaces [8,10,11]. Recently, the synthesis and physicochemical properties of hureaulite have garnered widespread attention in mineralogy and materials science [5,12–14]. In recent years, spectroscopic studies concerning phosphate minerals are increasing, especially due to their industrial and technological importance, however, only Near-infrared vibrational spectroscopic data are available on hureaulite [16].

Farmer [17] divided the vibrational spectra of phosphates according to the presence, or absence of water and hydroxyl units in the minerals. In aqueous systems, Raman spectra of phosphate oxyanions show a symmetric stretching mode (ν_1) at 938 cm^{-1}, the antisymmetric stretching mode (ν_3) at 1017 cm^{-1}, the symmetric bending mode (ν_2) at 420 cm^{-1} and the ν_4 mode at 567 cm^{-1} [18–20]. The value for the ν_1 symmetric stretching vibration of PO_4 units as determined by infrared spectroscopy was given as 930 cm^{-1} (augelite), 940 cm^{-1} (wavellite), 970 cm^{-1} (rockbridgeite), 995 cm^{-1} (dufrenite) and 965 cm^{-1} (beraunite). The position of the symmetric stretching vibration is mineral dependent and a function of the cation and crystal structure. The fact that the symmetric stretching mode is observed in the infrared spectrum affirms a reduction in symmetry of the PO_4 units.

The value for the ν_2 symmetric bending vibration of PO_4 units as determined by infrared spectroscopy was given as 438 cm^{-1} (augelite), 452 cm^{-1} (wavellite), 440 and 415 cm^{-1} (rockbridgeite), 455, 435 and 415 cm^{-1} (dufrenite) and 470 and 450 cm^{-1} (beraunite). The observation of multiple bending modes provides an indication of symmetry reduction of the PO_4 units. This symmetry reduction is also observed through the ν_3 antisymmetric stretching vibrations. Augelite shows infrared bands at 1205, 1155, 1079 and 1015 cm^{-1}; wavellite at 1145, 1102, 1062 and 1025 cm^{-1}; rockbridgeite at 1145, 1060 and 1030 cm^{-1}; dufrenite at 1135, 1070 and 1032 cm^{-1}; and beraunite at 1150, 1100, 1076 and 1035 cm^{-1}.

In the infrared study of triploidite, a basic manganese phosphate, Farmer reports the infrared spectrum with the (ν_1) at 957 cm^{-1}, (ν_3) at 1090, 1058, 1030 and 1010 cm^{-1}, (ν_2) at 420 cm^{-1} and the ν_4 mode at 595, 570, 486 cm^{-1} [12]. A hydroxyl stretching frequency of 3509 cm^{-1} was given. In the spectroscopic study of strengite, in the region below to 400 cm^{-1}, Frost and Weier [21] described the metal stretching vibrations for MnO and also the OMnO bending modes.

In this work, samples of a monomineral hureaulite from the Cigana pegmatite, located in the municipality of Conselheiro Pena, Minas Gerais, Brazil have been characterized. Studies include chemistry and backscattering images via SEM in the EDS mode and electron probe microanalysis in the WDS mode (EPMA), spectroscopic characterization of the structure with infrared and Raman.

2. Geological setting, occurrence and general appearance

The Cigana mine, located in the municipality of Conselheiro Pena, is a well-known pegmatite in Brazil, being an important source of rare phosphates. The pegmatite is located in the Conselheiro Pena pegmatite district, one of the subdivisions of the Eastern Brazilian Pegmatite province (EBP) [22]. The Conselheiro Pena pegmatite district covers an area of about 5000 km^2, in the middle part of the Doce River basin, about 360 km NE of the city of Belo Horizonte.

The Cigana mine in the past was mined for industrial feldspar and with minor importance gemstones and samples for the collectors market. The pegmatite is heterogeneous with well-developed mineralogical and textural zoning. It has symmetric lens shape with the longer axis trending to NW–SE and body dips sub vertically. The minimum extension is of about 50 m and 20 m thickness. The pegmatite is hosted by quartz–mica schist with garnet, staurolite and sillimanite of the São Tomé Formation. Tourmalinization is observed in the contact between the pegmatite and the host rock. Hydrothermal and metasomatic fluids were responsible for the albitization and development of miarolitic cavities, and a complex secondary phosphate assemblage was described by Chaves et al. [23].

The primary mineral association is represented by quartz, muscovite, microcline, schorl, almandine-spessartine, spodumene and triphylite. The secondary association is mainly composed by albite, Ta and Nb oxides, hydrothermal beryl, cassiterite, pyrite and a complex paragenesis of phosphates formed as a result of hydrothermal alteration of triphylite [23]. In the Cigana pegmatite, secondary phosphates, namely eosphorite, fairfieldite, fluorapatite, frondelite, gormanite, hureaulite, lithiophilite, reddingite and vivianite are common minerals in miarolitic cavities and in massive blocks formed after the aggregates of primary triphylite. Hureaulite crystals up to 5.0 mm along the *c* axis with monoclinic prismatic morphology occur in miarolitic cavities and after triphylite, in association with vivianite, lithiophilite and reddingite.

3. Experimental

3.1. Samples and preparation

Pink hureaulite single crystals from granitic pegmatite from Minas Gerais were obtained from the collection of the Geology Department of the Federal University of Ouro Preto, Minas Gerais, Brazil, with sample code SAA-081. The sample is from Cigana claim (also named Jocão claim), a lithium bearing pegmatite with triphylite and spodumene. The mine is located in Conselheiro Pena, east of Minas Gerais. To remove contaminate phases, with the support of a Stereomicroscope Leica Model EZ4, hureaulite crystals were handily selected from a sample in association with reddingite, lithiophilite, triphylite and vivianite. The hureaulite crystals were phase analyzed by X-ray powder diffraction and scanning electron microscopy in the EDS mode (SEM/EDS).

3.2. Scanning electron microscopy (SEM)

Hureaulite samples were coated with a thin layer of evaporated carbon. Secondary electron images and backscattering electron images were obtained using a JEOL-5510 scanning electron microscope (SEM) from the Geology Department of the Federal University of Ouro Preto. Qualitative chemical analysis by SEM in the EDS mode was produced to support the mineral characterization and determine the elements to be analyzed by Electron probe micro-analysis.

3.3. Electron probe micro-analysis (EPMA)

A quantitative chemical analysis was carried via EPMA. Hureaulite single crystal selected for this study was analyzed with the performance of five spots. The chemical analysis was carried out with a Jeol JXA8900R spectrometer from the Physics Department of the Federal University of Minas Gerais, Belo Horizonte. For each selected element was used the following standards: Fe – magnetite, Mg – olivine, Mn – rhodonite, P and Ca – Apatite Astimex, Al – Corundum and F – Fluorite. The epoxy embedded hureaulite sample was polished in the sequence of 9 μm, 6 μm and 1 μm diamond paste MetaDI® II Diamond Paste–Buhler, using water as a lubricant, with a semi-automatic MiniMet® 1000 Grinder–Polisher-Buehler. Finally, the epoxy embedded hureaulite was coated with a thin layer of evaporated carbon. The electron probe microanalysis in the WDS (wavelength dispersive spectrometer) mode was obtained at

15 kV accelerating voltage and beam current of 10 nA. Chemical formula was calculated on the basis of twenty oxygen atoms.

3.4. Raman microprobe spectroscopy

Crystals of hureaulite were placed on a polished metal surface on the stage of an Olympus BHSM microscope, which is equipped with 10×, 20×, and 50× objectives. The microscope is part of a Renishaw 1000 Raman microscope system, which also includes a monochromator, a filter system and a CCD detector (1024 pixels). The Raman spectra were excited by a Spectra-Physics model 127 He–Ne laser producing highly polarized light at 633 nm and collected at a nominal resolution of 2 cm^{-1} and a precision of ±1 cm^{-1} in the range between 200 and 4000 cm^{-1}. Repeated acquisitions on the crystals using the highest magnification (50×) were accumulated to improve the signal to noise ratio of the spectra. The spectra were collected over night. Raman Spectra were calibrated using the 520.5 cm^{-1} line of a silicon wafer. The Raman spectrum of at least 10 crystals was collected to ensure the consistency of the spectra.

3.5. Infrared spectroscopy

Infrared spectra were obtained using a Nicolet Nexus 870 FTIR spectrometer with a smart endurance single bounce diamond ATR cell. Spectra over the 4000–525 cm^{-1} range were obtained by the co-addition of 128 scans with a resolution of 4 cm^{-1} and a mirror velocity of 0.6329 cm/s. Spectra were co-added to improve the signal to noise ratio.

Spectral manipulation such as baseline correction/adjustment and smoothing were performed using the Spectracalc software package GRAMS (Galactic Industries Corporation, NH, USA). Band component analysis was undertaken using the Jandel 'Peakfit' software package that enabled the type of fitting function to be selected and allows specific parameters to be fixed or varied accordingly. Band fitting was done using a Lorentzian-Gaussian cross-product function with the minimum number of component bands used for the fitting process. The Gaussian-Lorentzian ratio was maintained at values greater than 0.7 and fitting was undertaken until reproducible results were obtained with squared correlations of r^2 greater than 0.995.

4. Results and discussion

4.1. Chemical characterization

The SEM/BSE images of hureaulite crystals studied in this work are shown in Fig. 1. The image shows hureaulite crystals up to 0.8 mm in length with monoclinic prismatic form. They occur in association with orthorhombic dipyramidal crystals of reddingite. The mineral association suggests that hureaulite grew after the crystallization of reddingite.

The quantitative chemical analysis of hureaulite is presented in Table 1. Composition is the result of medium values in five spots. H_2O content was calculated by stoichiometry and the chemical formula was calculated on the basis of 20 O atoms (O, OH, H_2O). The chemical composition indicates a Fe rich hureaulite as an intermediate member in a series between hureaulite and an unknown mineral. Chemical formula can be expressed as: $(Mn_{3.23}, Fe_{1.04}, Ca_{0.19}, Mg_{0.13})(PO_4)_{2.13}(OH)_{4.78}$.

4.2. Spectroscopy

The Raman spectrum of hureaulite in the 4000–100 cm^{-1} range is displayed in Fig. 2a. This figure shows the position and relative intensity of the bands in the Raman spectrum. It is obvious that there are large parts of the spectrum where no intensity is observed. The spectrum is therefore subdivided into sections based upon the particular vibrations being studied. The infrared spectrum of hureaulite in the 4000–500 cm^{-1} region is displayed in Fig. 2b. Again as for the Raman spectrum, the infrared spectrum is subdivided into sections based upon the type of vibration being studied. The Raman spectrum in the 1400–800 cm^{-1} region is reported in Fig. 3a and the infrared spectrum over the 1200–500 cm^{-1} region is shown in Fig. 3b. The results of the band component analysis of the Raman and infrared spectra are reported in Table 2.

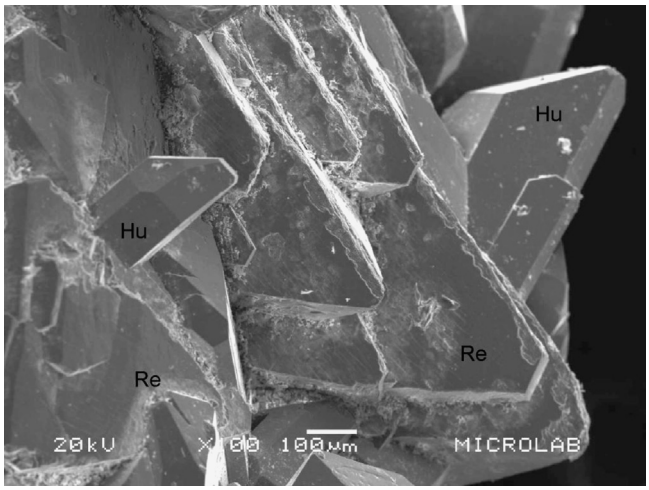

Fig. 1. SEM/BSE image of hureaulite (Hu) in association with reddingite (Re).

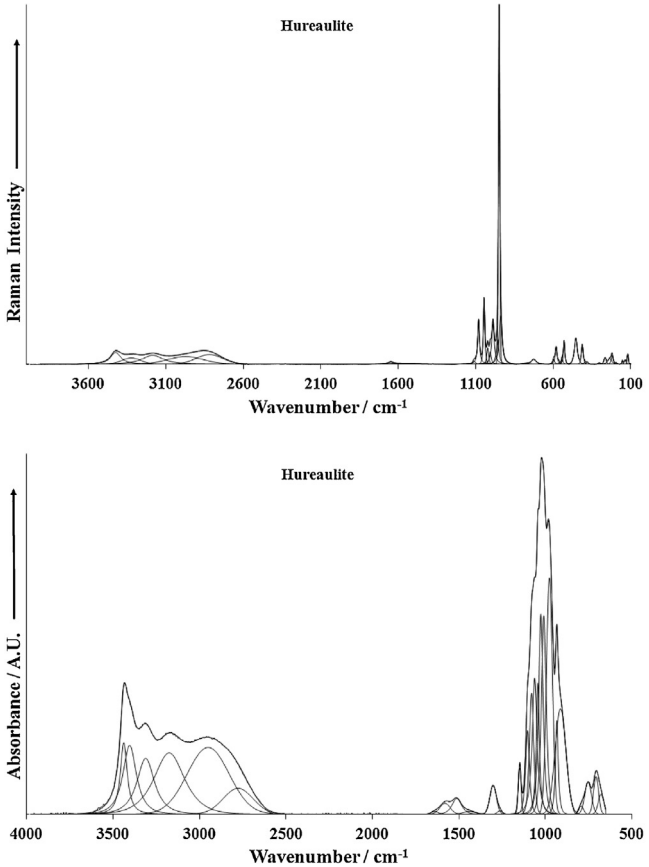

Fig. 2. (a) Raman spectrum of hureaulite over the 4000–100 cm^{-1} range and (b) infrared spectrum of hureaulite over the 4000–500 cm^{-1} range.

Table 1
Chemical composition of hureaulite from Cigana pegmatite (mean of 5 electron microprobe analyses). H_2O calculated by stoichiometry. Values in mass fraction/% (MF/%).

Constituent	(MF/%)	Number of cations	Range (MF/%)	Probe standard
MnO	32.93	3.23	32.69–33.46	Rhodonite
FeO	10.76	1.04	9.03–12.28	Magnetite
CaO	1.52	0.19	0.59–2.18	$Ca_2P_2O_7$
MgO	0.74	0.13	0.65–0.84	Olivine
P_2O_5	43.36	4.13	42.72–43.82	$Ca_2P_2O_7$
H_2O	12.36	4.78	Calculated by stoichiometry	
Total	101.67	11.50		

The Raman spectrum is noteworthy for a very intense band at 950 cm^{-1} which is assigned to the HPO_4^{2-} PO stretching vibrations. This band has a shoulder at 941 cm^{-1}. This band is given the same assignment, the implication of which is that all the hydrogen phosphate units are not equivalent. A low intensity Raman band is found at 989 cm^{-1} and is assigned to the phosphate PO_4^{3-} symmetric stretching vibration. Other Raman bands are observed at 1007, 1024, 1047, 1083 and 1109 cm^{-1}. These bands are assigned to the ν_3 antisymmetric stretching vibrations of the HPO_4^{2-} and PO_4^{3-} antisymmetric stretching vibrations.

The infrared spectrum of hureaulite (Fig. 3b) shows a complex spectral profile with a series of overlapping bands. The two infrared bands at 913 and 934 cm^{-1} are assigned to the HPO_4^{2-} PO symmetric stretching vibrations. The infrared bands at 977 and 1009 cm^{-1} are due to the PO_4^{3-} symmetric stretching vibrations. The intense infrared bands at 1026, 1044, 1062, 1080 1104 and 1149 are attributed to the HPO_4^{2-} and PO_4^{3-} antisymmetric stretching vibrations. The group of low intensity bands at 678, 797, 753 and 793 cm^{-1} are probably due to water librational modes.

The Raman spectrum of hureaulite in the 800–300 cm^{-1} and in the 300–100 cm^{-1} spectral range is displayed in Fig. 4a and 4b. The

Table 2
Results of the band component analysis of the Raman and infrared spectra of hureaulite.

Raman		IR	
Wavenumber	Assigned band	Wavenumber	Assigned band
3424	H_2O stretching	3439	H_2O stretching
3322	H_2O stretching	3405	H_2O stretching
3185	H_2O stretching		
		3312	H_2O stretching
		3176	H_2O stretching
2973	H_2O stretching	2951	H_2O stretching
2818	H_2O stretching	2778	H_2O stretching
1648	HOH bending	1640	HOH bending
		1581	
1571	ν_3 antisymmetric stretching of the $HPO_4^{2-}PO_4^{3-}$	1513	
		1440	
		1302	
		1263	
		1149	$\nu_3 HPO_4^{2-}$ and PO_4^{3-} antisymmetric stretching
1109		1104	ν_3 HPO_4^{2-} and PO_4^{3-} antisymmetric stretching
1083	ν_3 antisymmetric stretching of the $HPO_4^{2-}PO_4^{3-}$	1080	ν_3 HPO_4^{2-} and PO_4^{3-} antisymmetric stretching
1047	ν_3 antisymmetric stretching of the $HPO_4^{2-}PO_4^{3-}$	1062	ν_3 HPO_4^{2-} and PO_4^{3-} antisymmetric stretching
		1044	$\nu_3 HPO_4^{2-}$ and PO_4^{3-} antisymmetric stretching
1024	ν_3 antisymmetric stretching of the $HPO_4^{2-}PO_4^{3-}$	1026	ν_3 HPO_4^{2-} and PO_4^{3-} antisymmetric stretching
1007	ν_3 antisymmetric stretching of the HPO_4^{2-} ν_1 PO_4^{3-}	1009	PO_4^{3-} symmetric stretching
989	ν_1 PO_4^{3-}	977	PO_4^{3-} symmetric stretching
960			
950	ν_1 HPO_4^{2-} PO	934	HPO_4^{2-} PO
941	ν_1 HPO_4^{2-} PO	913	HPO_4^{2-} PO
778		793	H_2O
726		753	H_2O
		707	H_2O
		678	H_2O
598	ν_4 out of plane bending modes of the HPO_4 and PO_4		
582	ν_4 out of plane bending modes of the HPO_4 and PO_4		
564	ν_4 out of plane bending modes of the HPO_4 and PO_4		
543	ν_4 out of plane bending modes of the HPO_4 and PO_4		
531	ν_4 out of plane bending modes of the HPO_4 and PO_4		
455	ν_2 HPO_4 and PO_4 bending		
414	ν_2 HPO_4 and PO_4 bending		
398	MO bending		
381	MO bending		
304	MO bending		
267	External or lattice vibrations		
237	External or lattice vibrations		
221	External or lattice vibrations		
194	External or lattice vibrations		
155	External or lattice vibrations		
137	External or lattice vibrations		
120	External or lattice vibrations		

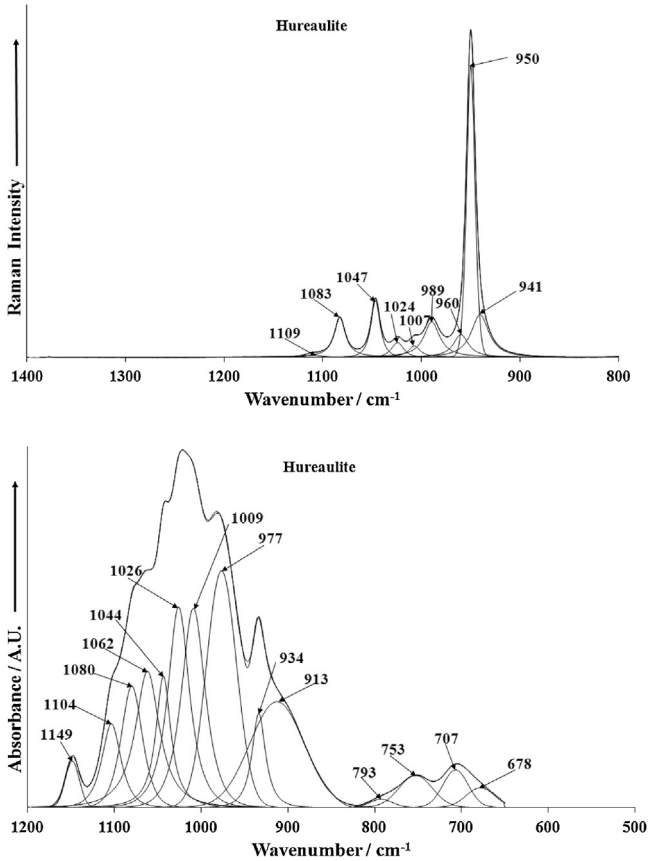

Fig. 3. (a) Raman spectrum of hureaulite over the 1400–800 cm^{-1} range and (b) infrared spectrum of hureaulite over the 1200–500 cm^{-1} range.

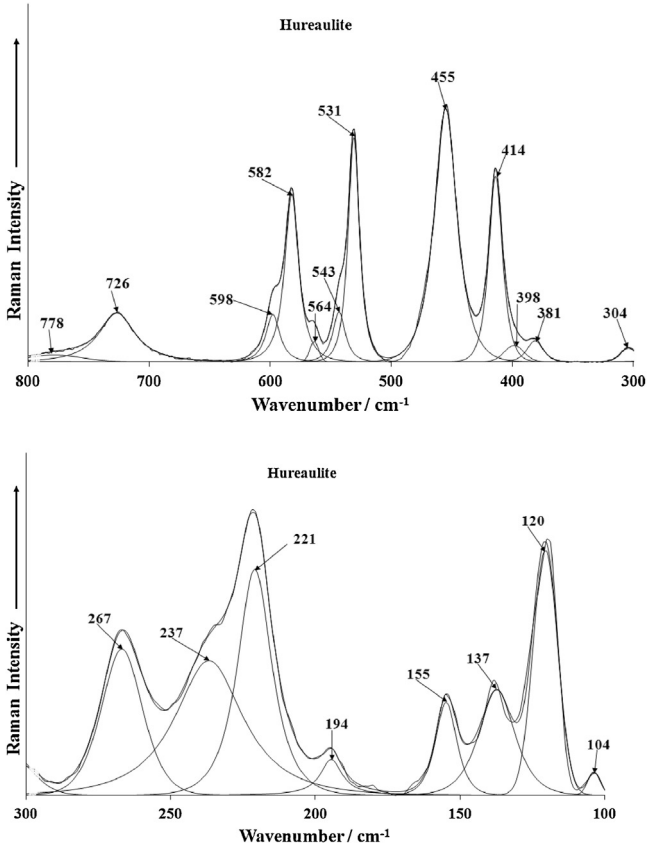

Fig. 4. (a) Raman spectrum of hureaulite over the 800–300 cm^{-1} region and (b) raman spectrum of hureaulite over the 300–100 cm^{-1} region.

series of bands at 531, 543, 564, 582 and 598 cm^{-1} are assigned to the ν_4 out of plane bending modes of the HPO_4 and PO_4, units. These bands were not observed in the infrared spectra. The Raman bands at 414 and 455 cm^{-1} are attributed to the ν_2 HPO_4 and PO_4 bending modes. The Raman bands at 304, 381, and 398 are attributed to MO bending modes. Strong Raman bands are observed at 120, 221 and 267 cm^{-1} with bands of lower intensity at 137, 155, 194 and 237 cm^{-1}. These bands are defined as external or lattice vibrations.

The Raman and infrared spectra over the 3800–2400 cm^{-1} spectral range are displayed in Fig. 5a and 5b, respectively. Raman bands are noted at 2818, 2973, 3185, 3322 and 3424 cm^{-1} and are assigned to water stretching vibrations. The number of water stretching vibrations proves that the water molecules in the hureaulite structure are not equivalent. Infrared bands are observed at 2778, 2951, 3176, 3312, 3405 and 3439 cm^{-1}. The infrared spectrum is similar in shape to the Raman spectrum. The significance of the position of the bands is related to the strength of the hydrogen bonds formed between the water and the phosphate and hydrogen phosphate units.

Studies have shown a strong correlation between OH stretching frequencies and both O···O bond distances and H···O hydrogen bond distances [24–27]. Libowitzky showed that a regression function can be employed relating the hydroxyl stretching wavenumbers with regression coefficients better than 0.96 using infrared spectroscopy [28]. The function is described as: $(\upsilon_1 = 3592 - 304 \times 10^9 \times \exp - (d(0-0)/0.1231)\ \ cm^{-1}$. Thus OH···O hydrogen bond distances may be calculated using the Libowitzky empirical function. Hydrogen bond distances may be obtained by using the OH stretching wavenumbers as given in Fig. 5. The values for the OH stretching vibrations shown in the Raman spectrum, provide hydrogen bond distances of 2.6140 Å (2818 cm^{-1}), 2.6436 Å (2973 cm^{-1}), 2.6989 Å (3185 cm^{-1}), 2.7532 Å (3322 cm^{-1}), 2.8158 Å (3424 cm^{-1}). By using the position of the infrared OH stretching wavenumbers as given in Fig. 5b. Here hydrogen bond distances are calculated as 2.6074 (2778 cm^{-1}), 2.6389 Å (2951 cm^{-1}), 2.6961 Å (3176 cm^{-1}), 2.7484 Å (3312 cm^{-1}), 2.8017 Å (3405 cm^{-1}), 2.8282 Å (3439 cm^{-1}). It is observed that the hydrogen bond distances calculated from the infrared spectra are in a similar range as calculated from the Raman spectrum.

The large hydrogen bond distances which are present in hureaulite can also be seen in other mixed anion minerals such as peisleyite and perhamite [29,30] where the distances ranging between 3.052(5) and 2.683(6) Å. Such hydrogen bond distances are typical of secondary minerals. A range of hydrogen bond distances are observed from reasonably strong to weak hydrogen bonding. This range of hydrogen bonding contributes to the stability of the mineral. Two types of OH units can be identified in the structure of hureaulite. The hydrogen bond distances previously established can be used to predict the hydroxyl stretching wavenumbers. The spectrum of hureaulite may be divided into two groups of OH stretching wavenumbers; namely 2600–3000 cm^{-1} and 3000–3600 cm^{-1}. This distinction suggests that the strength of the hydrogen bonds as measured by the hydrogen bond distances can also be divided into two groups according to the H-bond distances. An arbitrary cut-off point may be 2.6495 Å based upon the wavenumber 3000 cm^{-1}. Thus the bands listed above may be described as weak hydrogen bonds and the last bands as relatively strong hydrogen bonds.

The Raman spectrum of hureaulite in the 1800–1400 cm^{-1} spectral range is displayed in Fig. 6a. The infrared spectrum in the 1800–1200 cm^{-1} region is reported in Fig. 6b. It is noted that a single Raman peak is observed at 1648 cm^{-1} and is assigned to the water HOH bending mode. The position of the band gives a strong

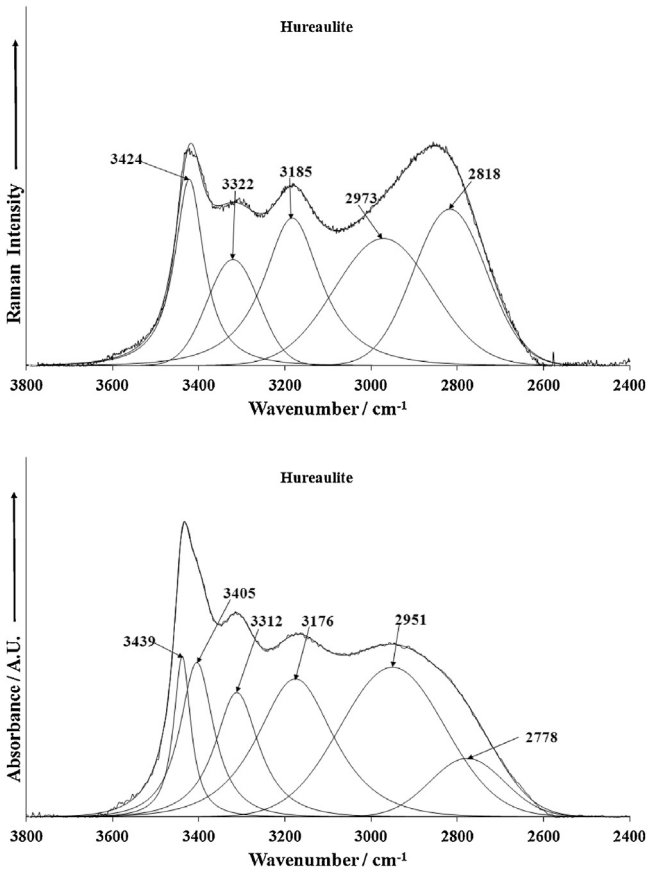

Fig. 5. (a) Raman spectrum of hureaulite over the 3800–2400 cm^{-1} range and (b) infrared spectrum of hureaulite over the 3800–2400 cm^{-1} range.

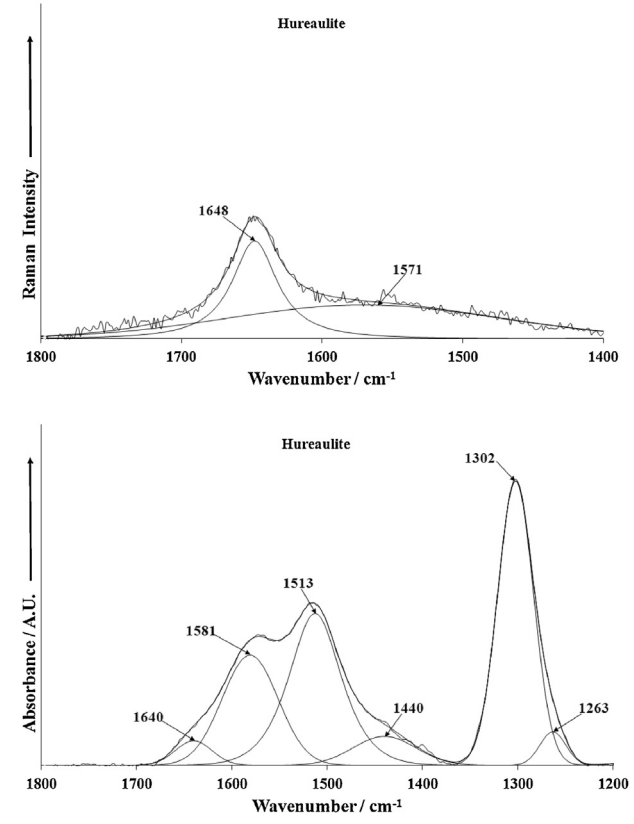

Fig. 6. (a) Raman spectrum of hureaulite over the 1800–1400 cm^{-1} range and (b) infrared spectrum of hureaulite over the 1800–1200 cm^{-1} range.

indication that the water is in a strong hydrogen bonded structure. The band is also observed in around this position in the infrared spectrum. The water bending band is observed at around 1620 cm^{-1} for liquid water and 1595 cm^{-1} for water vapour. If the water is strongly hydrogen bonded, then the band is observed at higher wavenumbers as is the case in these spectra. The band for strongly hydrogen bonded water might be observed at around 1650 cm^{-1}.

5. Conclusions

An iron rich hureaulite was studied by Electron Micro-Probe in the WDS mode, Raman and infrared spectroscopy. The chemical analysis shows chemical formula expressed by $(Mn_{3.23}, Fe_{1.04}, Ca_{0.19}, Mg_{0.13})(PO_4)_{2.7}(HPO_4)_{2.6}(OH)_{4.78}$, that indicate predominance hureaulite member in a series between hureaulite and a Fe unknown member. This solid solution was confirmed by studies carried out by Moreira et al. [8] in the synthesis of Fe compounds with hureaulite structure. Traces of Ca and Mg were also found in substitution of Mn in the octahedral site. SEM/BSE images of hureaulite crystals in association with reddingite suggests that hureaulite grew after the crystallization of reddingite.

Aspects of the structure of hureaulite using vibrational spectroscopy were assessed. Raman and infrared bands associated with hydrogen phosphate and phosphate units were observed. It is apparent that all three anion types exist in the structure of hureaulite and these anionic types are enhanced by the basic nature of the mineral. The proton on the water units is apparently very mobile and enables the formation of the monohydrogen and dihydrogen phosphate units.

Acknowledgements

The financial and infra-structure support of the Discipline of Nanotechnology and Molecular Science, Science and Engineering Faculty of the Queensland University of Technology, is gratefully acknowledged. The Australian Research Council (ARC) is thanked for funding the instrumentation. R. Scholz thanks to FAPEMIG – Fundação de Amparo à Pesquisa do Estado de Minas Gerais (grant No. CRA – APQ-03998-10).

References

[1] F. Alluaud, Ann. Sci. Nat. 8 (1826) 334.
[2] A. Dufrénoy, Ann. Chim. Phys. 41 (1829) 337.
[3] A.R. Kampf, Am. Mineral. 94 (2009) 1535.
[4] P. Elliott, P. Turner, P. Jensen, U. Kolitsch, A. Pring, Mineral. Mag. 73 (2009) 723.
[5] R. Pierrot, B. Soc. Fr. Mineral. Cr. 87 (1964) 169.
[6] H. Sarp, Schweiz. Miner. Petrogr. 64 (1984) 323.
[7] P.B. Moore, T. Araki, Am. Mineral. 58 (1973) 302.
[8] L.F. Moreira, P.H. Domingues, E. Mattievich, J. Magn. Magn. Mater. 132 (1994) 191.
[9] P.B. Moore, Mineral. Rec. 4 (1973) 103.
[10] A.M. Chippindale, F.O.M. Gaslain, A.D. Bond, A.V. Powell, J. Mater. Chem. 13 (2003) 1950.
[11] K. Nomura, Y. Ujihira, J. Mater. Sci. 17 (1982) 3437.
[12] K. Nomura, Y. Ujihira, Nippon Kagaku Kaishi (1982) 1352.
[13] G. Qiu, H. Yin, F. Liu, X. Feng, W. Tan, M. Liu, X. Chen, Huazhong Agricultural University, Peop. Rep. China, Application: CN 2010, p 11.
[14] G.-H. Qiu, Z.-Y. Gao, H. Yin, X.-H. Feng, W.-F. Tan, F. Liu, Solid State Sci. 12 (2010) 808.
[15] H. Yin, F. Liu, X. Chen, X. Feng, W. Tan, G. Qiu, Microporous Mesoporous Mater. 153 (2012) 115.
[16] R.L. Frost, K.L. Erickson, Spectrochim. Acta A 61 (2005) 45.
[17] V.C. Farmer, The Infrared Spectra of Minerals, Monograph 4, 1st ed., Mineralogical Society, London, 1974.
[18] R.L. Frost, W. Martens, P.A. Williams, J.T. Kloprogge, J. Raman Spectrosc. 34 (2003) 751.
[19] R.L. Frost, W. Martens, P.A. Williams, J.T. Kloprogge, Mineral. Mag. 66 (2002) 1063.
[20] R.L. Frost, W.N. Martens, T. Kloprogge, P.A. Williams, Neues Jb. Miner. Monat. (2002) 481.

[21] R.L. Frost, M.L. Weier, J. Mol. Struct. 697 (2004) 207.
[22] A.C. Pedrosa-Soares, C.M.d. Campos, C.M. Noce, L.C.d. Silva, T.A. Novo, J. Roncato, S.M. Medeiros, C. Castañeda, G.N. Queiroga, E. Dantas, I.A. Dussin, F. Alkmim, Geol. Soc. Spec. Publ. 350 (2011) 25.
[23] M.L.S.C. Chaves, R. Scholz, D. Atencio, J. Karfunkel, Geociências 24 (2005) 143.
[24] J. Emsley, Chem. Soc. Rev. 9 (1980) 91.
[25] H.D. Lutz, Struct. Bond. 82 (1995) 85.
[26] W. Mikenda, J. Mol. Struct. 147 (1986) 1.
[27] A. Novak, Struct. Bond. 18 (1974) 177.
[28] E. Libowitsky, Monatsh. Chem. 130 (1999) 1047.
[29] R.L. Frost, S.J. Mills, M.L. Weier, Spectrochim. Acta A 61 (2004) 177.
[30] R.L. Frost, M.L. Weier, S.J. Mills, Spectrochim. Acta A 67 (2007) 604.